Direct-detection OFDM-QPSK system performance improvement enabled by DFT spread and receiver-based ISFA algorithm

Jie Su (苏 婕)*, Xinying Li (李欣颖), and Jianjun Yu (余建军)

Education Ministry Key Laboratory of Electromagnetic Wave Information Science, Information Science and Engineering School, Fudan University, Shanghai 200433, China

**Corresponding author: jiesu12@fudan.edu.cn*

Received October 12, 2015; accepted March 11, 2016; posted online April 21, 2016

We experimentally demonstrate a direct-detection orthogonal-frequency-division-multiplexing quadrature-phase-shift-keying (OFDM-QPSK) system that is capable of delivering a 32 Gbaud OFDM-QPSK signal over 7 km single-mode fiber-28 (SMF-28). Intra-symbol frequency-domain averaging (ISFA) channel response estimation is applied to suppress in-band noise, while discrete Fourier transform-spread (DFT-spread) is used to reduce the peak-to-average power ratio (PAPR) of the transmitted OFDM signal. With the aid of ISFA-based channel estimation and PAPR reduction enabled by DFT-spread, the bit-error ratio of the system after 7 km SMF-28 transmission can be improved from 2×10^{-3} to error-free when the received optical power is -8.5 dBm.

OCIS codes: 060.0060, 060.2330, 060.4510, 060.5060, 060.4370.

doi: 10.3788/COL201614.050608.

Recently, with the rapid development of Internet applications, conventional short-reach optical communication systems that use direct-detection (DD) and wavelength division multiplexing are now unable to fulfill the increasing demands on capacity. As a result, the core need of current optical communication systems is finding a way to increase the system capacity and thus to realize high spectral efficiency transmission. Orthogonal frequency division multiplexing (OFDM) has been regarded as one of the core technologies for a next generation communication system because of high frequency spectrum utilization. A DD-OFDM system with a simple architecture has recently received much attention and has been actively investigated in short-reach optical communications[1–3].

In this Letter, we have experimentally demonstrated a DD OFDM quadrature-phase-shift-keying (QPSK) system that is capable of delivering a 32 Gbaud OFDM-QPSK signal over 7 km single-mode fiber-28 (SMF-28). The system performance improvement was enabled by discrete Fourier transform-spread (DFT-spread) and the receiver-based intra-symbol frequency domain averaging (ISFA) algorithm. The experimental result showed that after 7 km SMF-28 transmission, the bit-error ratio (BER) of a 32 Gb/s OFDM-QPSK signal at -8.7 dBm received optical power is improved from 2×10^{-3} to error-free with ISFA and DFT-spread.

A conventional DD-OFDM system structure[4,5] is shown in Fig. 1.

At the transmitter, an optical carrier is directly modulated by a real-value electrical OFDM signal via a Mach–Zehnder modulator (MZM). At the receiver, the amplitude of the optical signal is detected by a photodiode (PD) to obtain the electric OFDM signal.

OFDM is a special kind of multi-carrier modulation technology. However, the major drawback is that its signal waveform has a high peak-to-average power ratio (PAPR). The high PAPR will increase the processing burden of the analog-to-digital converter (ADC), amplifier, and modulator, and thus lead to system performance degradation. There are many PAPR reduction techniques for OFDM transmission[6–11]. In the OFDM system, the autocorrelation function of the input data sequence is closely related to the PAPR[9]. It can be defined as

$$\mathrm{PAPR} \le 1 + \frac{2}{N} \cdot \sum_{k=1}^{N-1} |R_k|, \tag{1}$$

where $\sum_{K=1}^{N-1} |R_k|$ is the aperiodic autocorrelation function of the input data sequence. We can see from Eq. (1) that

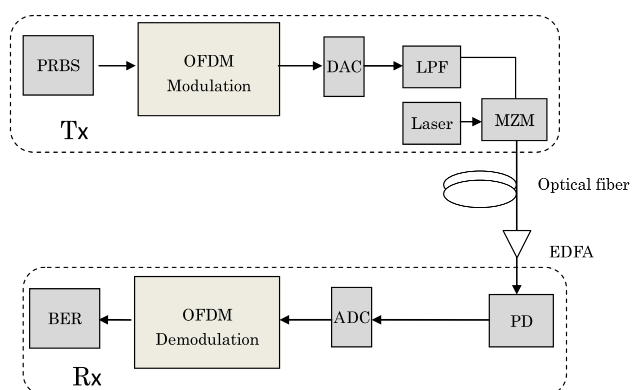

Fig. 1. System structure of conventional DD-OFDM (Tx, transmitter, Rx, receiver; PRBS, pseudo random bit sequence; DAC, digital-to-analogue conversion; LPF, low-pass filter; EDFA, erbium-doped fiber amplifier).

when its sum is reduced, the PAPR will be reduced. The DFT-spread technology can effectively improve the PAPR performance by reducing the sum in Eq. (1)[10]. The modulation and demodulation principle of a DFT-spread OFDM signal is shown in Fig. 2. Compared to the conventional OFDM modulation, the inverse DFT (IDFT) is added before the inverse fast Fourier transformation (IFFT) function in DFT-spread OFDM modulation. The input signal is formed to a new DFT matrix by IDFT. The autocorrelation function of the input signal sequence can be reduced this way. The value of PAPR can be reduced accordingly. For the DFT-spread OFDM demodulation, a series of inverse processing procedures are carried out[7–11].

Accurate channel estimation is the key factor to improve the quality of the received signal and is also primarily a way to improve system performance. The purpose of the channel estimation is to obtain the channel response in the frequency domain and thus to ensure the correct recovery of the received data. In the DD-OFDM system, performance degradation of the system is mainly caused by the noise of the PD. ISFA technology improves the channel estimation by suppressing the noise[12–14].

The ISFA algorithm estimates the frequency response of a channel by utilizing training sequences (TSs). At the transmitter, a training symbol is inserted into the OFDM signal in a TS cycle. At the receiver, the channel characteristics are calculated according to the training symbols and the known training symbols after transmission. The channel matrix of received training symbols can be expressed as[12]

$$\begin{bmatrix} a(k) & b(k) \\ c(k) & d(k) \end{bmatrix} = \begin{bmatrix} t'_{1x}(k)/t_x(k) & t'_{2x}(k)/t_y(k) \\ t'_{1y}(k)/t_x(k) & t'_{2y}(k)/t_y(k) \end{bmatrix}, \quad (2)$$

where t_x and t_y are two training symbols, preferably with low PAPR. The known training symbols after transmission are t'_{1x}, t'_{1y}, t'_{2x}, and t'_{2y} in Eq. (2).

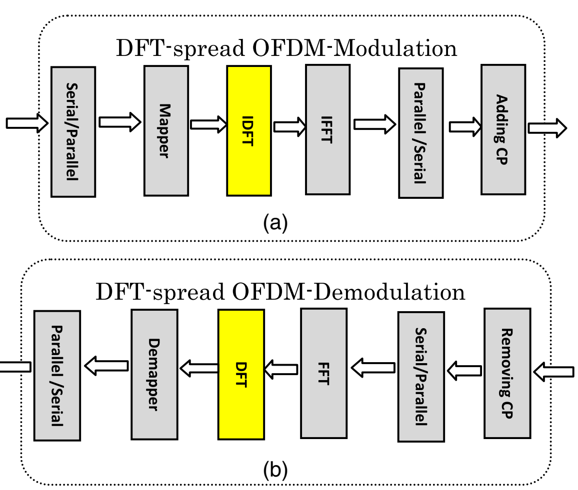

Fig. 2. Principle of DFT-spread OFDM modulation and demodulation.

According to Eq. (2), the channel matrix of each modulated subcarrier is the average of its own and its adjacent subcarrier channel matrix in the ISFA process. Typically, for subcarrier k, the averaging can be performed over subcarrier k and its "m" left neighbors and/or "m" right neighbors, or totally up to $(2m+1)$ adjacent subcarriers[12]. The improved channel matrix for subcarrier k' after the ISFA process can be expressed as[12]

$$\begin{bmatrix} a(k') & b(k') \\ c(k') & d(k') \end{bmatrix}_{\text{ISFA}} = \frac{1}{\min(k_{\max}, k'+m) - \max(k_{\min}, k'-m) + 1} \times \sum_{k=k'-m}^{k'+m} \begin{bmatrix} a(k) & b(k) \\ c(k) & d(k) \end{bmatrix}. \quad (3)$$

According to Eq. (3), the channel characteristics of the data symbols are estimated based on the channel characteristics of the training symbols.

The experimental setup for the 32 Gbaud OFDM-QPSK signal transmission utilizing single-arm MZM in a DD system is given in Fig. 3. At the transmitter, the optical carrier generated from a commercial external cavity laser (ECL) is externally modulated by an electrical 32 Gbaud OFDM-QPSK signal. The electrical OFDM signal is generated off-line in MATLAB and then uploaded into an arbitrary waveform generator (AWG) with a 64 GSa/s sample rate and 13 GHz bandwidth. In this experiment, the number of OFDM subcarriers is 256. Among these subcarriers, 198 of them are used to carry data. In addition, the first subcarrier is set to zero for DC-bias, and the rest (57) null subcarriers at the edge are reserved for oversampling. Since Hermitian symmetry is employed, only 99 of the 198 data subcarriers carry effective data. QPSK is employed for the subcarrier modulation scheme. A 32-point cyclic prefix (CP) is added into each OFDM symbol after IFFT. A TS, including one OFDM symbol, is added before every 50 OFDM symbols to assist channel estimation at the receiver. A TS and its subsequent 50 OFDM symbols compose one OFDM frame. In addition, 1000-point zeros are added before each OFDM frame to assist time synchronization at the receiver. The

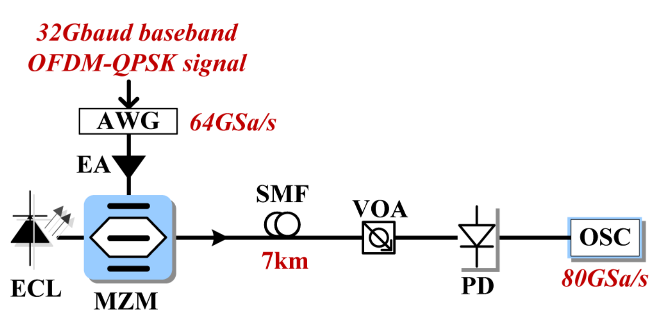

Fig. 3. Experimental setup for a 32 Gbaud OFDM-QPSK signal with 7 km SMF-28 transmission utilizing single-arm MZM in DD system (EA, electrical amplifier; OSC, oscilloscope).

continuous-wavelength light wave from ECL is modulated by an MZM driven by an electrical baseband OFDM signal. The 32 Gbaud total bit rate corresponds to an effective bit rate of 20.6 Gb/s $(32 \times (99/288) \times [(50 \times 288)/(1000 + 50 \times 288)] \times 2 \approx 20.6$ Gb/s). After 7 km SMF-28 transmission, the modulated signal is received by a PD. Variable optical attenuator (VOA) is placed before the PD to adjust the received optical power for sensitivity measurement. At the receiver, a QPSK-OFDM signal is obtained by a real-time oscilloscope with an 80 GSa/s sample rate and 30 GHz analog bandwidth. Subsequently, it can be processed by off-line digital signal processing (DSP). The off-line DSP includes CP removal, fast Fourier transformation, channel estimation with ISFA, one-tap equalization, de-mapping, DFT, and BER calculation. The BER is calculated by error counting over 10×10^6 bits (10 data sets with each set containing 10^6 bits).

Figure 4 gives the constellation comparison of 32 Gbaud QPSK after 7 km SMF-28 transmission when the input power into PD is −6.5 dBm. It can be seen that with the aid of ISFA, the constellation diagram of receive signal is more convergent, and the system performance is better at the same condition of receive power and BER.

When the received power of the PD is further reduced to −8.7 dBm, the performance of the system is decreased. Figure 5 gives the constellation comparison of 32 Gbaud QPSK after 7 km SMF-28 transmission when the input power into the PD is −8.7 dBm utilizing different technologies. It can be seen that with the aid of the ISFA algorithm, BER performance of the system can be improved

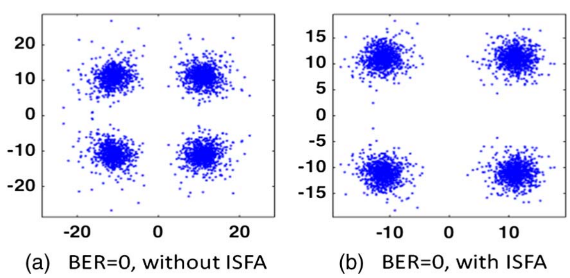

Fig. 4. Constellation comparison of a 32 Gbaud QPSK after 7 km SMF-28 transmission when the input power into the PD is −6.5 dBm.

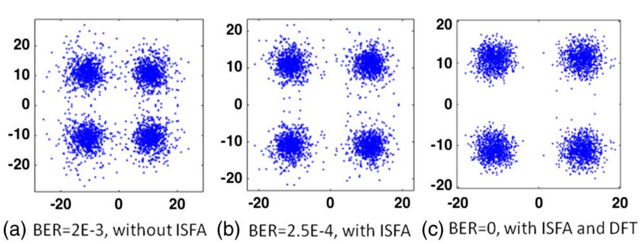

Fig. 5. Constellation comparison of a 32 Gbaud QPSK after 7 km SMF-28 transmission when the input power into the PD is −8.7 dBm utilizing different technologies.

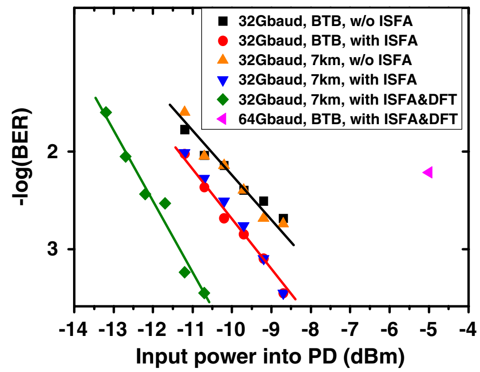

Fig. 6. Curves of BER versus input power into a PD utilizing different techniques.

from 2×10^{-3} to 2.5×10^{-4}. When using both ISFA and DFT-spread technology, the constellation is obviously more convergent, and the system performance is greatly improved. In this case, the BER performance of the system can be improved from 2×10^{-3} to error-free.

Curves of BER versus input power into the PD utilizing different technologies are shown in Fig. 6. The w/o in Fig. 6 represents the implementation with/without the ISFA algorithm. All the first four cases shown in Fig. 6 do not adopt DFT-spread. The measurements are given with the received optical power from −8 to −13 dBm in both back-to-back and after 7 km SMF-28. We can see that 7 km SMF-28 transmission causes no power penalty. Moreover, at the BER of 3.8×10^{-3} [corresponding to–log (BER) of 2.42] and a 32 Gbaud baud rate, the adoption of the ISFA algorithm improves receiver sensitivity by ∼1 dB, and the adoption of DFT-spread technology further improves the receiver sensitivity by ∼2 dB. When the baud rate is increased to 64 Gbaud, the BER performance is worse even when both the ISFA algorithm and DFT-spread technology are adopted, which is mainly because of the limited bandwidth of the optical and electrical components adopted in our experiment.

In conclusion, we experimentally demonstrate a DD OFDM-QPSK system that is capable of delivering a 32 Gbaud QPSK-OFDM signal over 7 km SMF-28. After 7 km SMF-28 transmission, the BER of system is improved from 2×10^{-3} to error-free with ISFA and DFT at −8.7 dBm received optical power. We find that the BER performance of the system is improved by DFT-spread and the receiver-based ISFA algorithm.

References

1. J. Armstrong, J. Lightwave Technol. **27**, 189 (2009).
2. H. Chen, F. Li, J. Xiao, Z. Cao, and J. Yu, J. Optoelectron. Laser **22**, 1057 (2011).
3. L. Peng, "Research on the Synchronization Algorithm of Direct Detection Optical OFDM System," Ph.D. Dissertation (Hunan University, 2013).
4. M. Chen, J. He, Z. Cao, J. Tang, and L. Chen, Opt. Commun. **326**, 80 (2014).
5. Q. Zhang, E. Hugues-Salas, Y. Ling, H. Zhang, R. Giddings, J. Zhang, M. Wang, and J. Tang, Opt. Express **22**, 6339 (2014).
6. S. Han and J. Lee, IEEE Trans. Wireless Commun. **12**, 56 (2005).

7. F. Zeng, L. Liu, H. Chen, and J. Yang, J. Terahertz Sci. Electron. Inf. Technol. **13**, 71 (2015).
8. R. Deng, Q. Fan, H. Dong, J. He, and L. Chen, J. Optoelectron. Laser **26**, 877 (2015).
9. C. Tellambura, Electron. Lett. **33**, 1608 (1997).
10. X. Zhu, G. Zhu, and P. Lin, Comput. Eng. Sci. **3l**, 109 (2009).
11. F. Li, J. Yu, Y. Fang, Z. Dong, and X. Ying, Opt. Express **22**, 8742 (2014).
12. X. Liu and F. Buchali, Opt. Express **16**, 21944 (2008).
13. M. Chen, J. He, and L. Chen, J. Opt. Commun. Netw. **6**, 18 (2014).
14. X. Zeng, J. Liu, J. Wang, L. Jia, and J. Gao, J. Optoelectron. Laser **25**, 1481 (2014).